# Subsonic and Supersonic Boundary-Layer Flow past a Wavy Wall

G. R. INGER*
*Virginia Polytechnic Institute and State University, Blacksburg, Va.*
AND
E. P. WILLIAMS†
*McDonnell Douglas Astronautics Company, Huntington Beach, Calif.*

**Steady two-dimensional compressible turbulent boundary-layer flow past a slightly wavy wall is studied both analytically and experimentally in the Mach number range $0.8 \leqq M_e \leqq 1.8$ at unit Reynolds numbers on the order of $10^6$ per inch. The measured and predicted wall pressure distributions are in good agreement and indicate that the nonuniform flow in the boundary layer can produce essentially a subsonic type of wall pressure signature ($p_{max}$ in valleys) in the presence of moderately supersonic inviscid flows. An interesting cusping of the pressure is also observed in the transonic regime. Measurements of the wall temperature perturbations are also made; the results agree with theory in showing a strong correlation between $T_{max}$ and $P_{max}$.**

## 1. Introduction

ASIDE from its fundamental interest, the problem of steady compressible boundary-layer flow past a two-dimensional wavy wall is of practical importance in engineering studies of surface disturbance effects on high speed boundary-layer separation and heating,[1,2] transonic flow[3] and ablation surface cross-hatching.[4] Moreover, while there is no direct application to unsteady phenomena such as panel flutter and hydrodynamic stability of liquid surfaces[5] the results nevertheless provide valuable insight to the effects of nonuniform boundary layer flow in these applications. Since in practice the boundary layer is often turbulent, studies of the problem have concentrated in this case. A previous experimental and theoretical investigation for a limited range of supersonic Mach numbers (1.2–1.7) and unit Reynolds numbers around $10^5$ per inch has been described by McClure.[6] In the present paper, a wider range of Mach numbers including the transonic range $0.8 \leqq M_e \leqq 1.8$ is considered at higher unit Reynolds numbers ($10^6$/in.) more representative of actual flight conditions. Moreover, in addition to the usual wall pressure measurements and theory, a theoretical and experimental study of the corresponding temperature perturbations is described.

In Sec. 2, a linearized theory of compressible nonuniform flow past a slightly wavy wall is presented, including the temperature and heat-transfer perturbation aspects of the flow. It is shown that the pressure field may be treated as an equivalent initial value (instead of a two point boundary value) problem and hence calculated very simply by direct inward integration across any given boundary-layer profile. In Sec. 3, the experimental set up is described including details of the wavy wall configuration and its instrumentation. The use of temperature sensitive liquid crystal paint as a means of measuring the surface temperature distribution is also discussed. Section 4 presents the resulting pressure and temperature measurements and comparisons with our theoretical predictions.

Received August 30, 1971; revision received January 12, 1972. This paper is based on work jointly supported by the U.S. Air Force under contract F04701-68-C-0288 and the McDonnell Douglas Astronautics Co. Independent Research and Development Program.

Index categories: Boundary Layers and Convective Heat Transfer—Turbulent; Subsonic and Transonic Flow.

* Professor of Aerospace Engineering. Associate Fellow AIAA.

† Senior Staff Engineer, Special Aerodynamic Problems. Associate Fellow AIAA.

## 2. Theoretical Analysis

The analysis is based on a parallel shear flow model of the undisturbed boundary layer and a linearized treatment of the small perturbation field wherein the solution is decomposed into a "slowly-varying" inviscid part which determines the pressure and a "rapidly-varying" viscous part that is important near the wall. The pressure field is analyzed first, including some important new thermodynamic aspects of the inviscid disturbance field. The effects of viscosity and heat conduction are then considered by extending earlier work in viscous sublayer effects in perturbed boundary-layer flows.

### 2.1 General Considerations

We assume steady compressible boundary-layer flow of a perfect gas with unit Prandtl number, subjected to steady perturbations sufficiently small that they may be treated by linearized theory (transonic or hypersonic mean flows are thereby excluded). Following Lighthill[7] and Benjamin[9] the mean flow is idealized in the first approximation as a inviscid plane parallel shear flow in the $x$ direction with uniform static pressure $p_\infty$ and arbitrary lateral variations of density $\rho_o(y)$, velocity $U_o(y)$, Mach number $M_o(y)$ and temperature $T_o(y)$. The perturbations are caused by the rippled surface $y_w(x) = \varepsilon \sin \alpha x$ (Fig. 1) where $\varepsilon$ is amplitude and $\alpha = 2\pi/\lambda$ the reciprocal wave length. Consequently the flow properties may be expressed as the sum of a mean value and a small perturbation harmonic in $\alpha x$; denoting $E \equiv \exp(i\alpha x)$ we thus write $U = U_o(y) + E\tilde{U}(y)$, $V = E\tilde{V}(y)$, $p = p_\infty + E\tilde{P}(y)$, $\rho = \rho_o(y) + E\tilde{R}(y)$ and $T = T_o(y) + E\tilde{T}(y)$ where it is understood that only the real parts of these complex quantities are of ultimate physical interest. Then substituting these expressions into the compressible Navier-Stokes equations, applying the aforementioned simplifying assumptions and retaining only first order

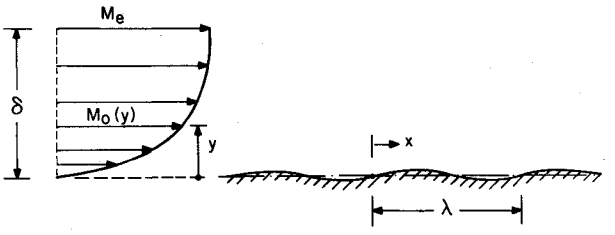


**Fig. 1 Flow configuration (schematic).**

perturbations, one obtains the following ordinary differential equations governing the perturbation distribution functions, $\tilde{U}$, $\tilde{V}$, $\tilde{P}$, etc.

$$i\alpha(\rho_o \tilde{U} + U_o \tilde{R}) + d(\rho_0 \tilde{V})/dy = 0 \tag{1}$$

$$i\alpha\rho_o U_o \tilde{U} + \rho_o \frac{dU_o}{dy}\tilde{V} + i\alpha\tilde{P} = \frac{d}{dy}\left[\mu_o\left(\frac{d\tilde{U}}{dy} + i\alpha\tilde{V}\right)\right] + \frac{d}{dy}\left(\tilde{\mu}\frac{dU_o}{dy}\right) - \frac{2}{3}\mu_o\left(i\alpha\frac{d\tilde{V}}{dy} + 2\tilde{U}\alpha^2\right) \tag{2}$$

$$i\alpha\rho_o U_o \tilde{V} + \frac{d\tilde{P}}{dy} = \frac{4}{3}\frac{d}{dy}\left[\mu_o\left(\frac{d\tilde{V}}{dy} - \frac{i\alpha}{2}\tilde{U}\right)\right] + i\alpha\frac{dU_o}{dy}\tilde{\mu} + \mu_o\left(i\alpha\frac{d\tilde{U}}{dy} - \alpha^2\tilde{V}\right) \tag{3}$$

$$i\alpha\rho_o U_o \tilde{H} + \rho_o \frac{dU_o}{dy}\tilde{V} = \frac{d}{dy}\left[\mu_o\left(\frac{d\tilde{H}}{dy} + i\alpha U_o \tilde{V}\right) + \tilde{\mu}\frac{dH_o}{dy}\right] + i\alpha\mu_o\frac{dU_o}{dy} - \tilde{U}\frac{d}{dy}\left(\mu_o\frac{dU_o}{dy}\right) - \mu_o\alpha^2(\tilde{H} + \tfrac{1}{3}U_o\tilde{U} + \tfrac{2}{3}U_o\tilde{V}) \tag{4}$$

$$\tilde{R} = \rho_o[(\tilde{P}/P_\infty) - (\tilde{T}/T_o)] \tag{5}$$

where $\mu_o$ and $\tilde{\mu}$ are the mean and perturbation effective viscosities, respectively, and where the energy equation (4) has been written in terms of the mean total enthalpy $H_o = C_p T_o + (U_o^2/2)$ and its perturbation $\tilde{H} = C_p\tilde{T} + U_o\tilde{U}$.

The formulation is completed by a specification of the boundary conditions. Consider first the outer edge $y = \delta$ of the boundary layer where the mean flow gradients vanish. Here the viscous effects on the perturbation field vanish exponentially[10] while the inviscid solutions are bounded and free from any externally imposed disturbances such as inward-running shock waves. Thus we have

$$\tilde{H}(\delta) = 0 \tag{6}$$

$$(d\tilde{P}/dy)(\delta) = -i(M_e^2 - 1)^{1/2}\tilde{P}(\delta) \tag{7}$$

which imply, respectively, that the perturbations become adiabatic and that the corresponding pressure field involves either simple Mach waves ($M_e > 1$) or exponentially decaying signals ($M_e < 1$). Now consider the inner boundary conditions on the wall when there is no mass transfer. Taking viscous and heat conduction effects into account, we impose $v'(0) = 0$ and the no slip condition $u(y_w) = 0 = u'(0) + \varepsilon(dU_o/dy)_w$ which yield

$$\tilde{V}(0) = 0 \tag{8}$$

$$\tilde{U}(0) = i\varepsilon\frac{dU_o}{dy}(0) \tag{9}$$

plus the conditions of either fixed surface temperature or heat transfer:

$$\tilde{H}(0) = i\varepsilon\frac{dH_o}{dy} \tag{10a}$$

or

$$\frac{d\tilde{H}}{dy}(0) = -\frac{\tilde{\mu}(0)}{\mu_o(0)}\frac{dH_o}{dy}(0) \tag{10b}$$

These wall boundary conditions must be replaced by an alternative set of conditions when only the inviscid part of the perturbation solution is sought, as discussed below.

### 2.2 Inviscid Solutions

Consider now the inviscid part of the disturbance field determined by discarding the viscous terms on the right hand sides of Eqs. (2–4). Lighthill[7] has shown from these equations that the pressure field $\tilde{P}$ can be described independently of the velocity, density and temperature by the following second order linear differential equation involving only the mean flow Mach number profile:

$$\left\{\frac{d^2}{dy^2} - 2\left(\frac{dM_o/dy}{M_o}\right)\frac{d}{dy} + \alpha^2(M_o^2 - 1)\right\}\tilde{P} = 0 \tag{11}$$

Once the equation is solved, the corresponding inviscid velocity and enthalpy perturbations follow directly from Eqs. (2–4). In particular, Eq. (4), which has not been discussed heretofore, yields the interesting result that

$$\tilde{H}(y)_{\text{inviscid}} = [(dH_o/dy)/\alpha]i(\tilde{V}/U_o)(y) \tag{12}$$

which shows that the inviscid total enthalpy perturbation is proportional to the local mean flow enthalpy gradient and the local perturbed streamline slope with a maximum in the streamline valleys (i.e., $\tilde{H}$ leads $\tilde{V}$ by $\pi/2$).

The solution of Eq. (11) must satisfy the outer boundary conditions (7); the proper inner boundary condition to use, however, requires some care since the solution is singular at $y = 0$ where $M_o \to 0$.[7,8] This difficulty can be avoided by imposing the kinematic tangency condition $v' = U_o(dy_w/dx) = \varepsilon\alpha U_o(y_f)$ for a wavy wall at some $y_f > 0$ above the actual surface; thus, substituting $\tilde{V} = \varepsilon\alpha U_o$ into the inviscid form of Eq. (3), one finds the effective inner inviscid boundary condition

$$(d\tilde{P}/dy)(y_f)_{\text{inviscid}} = -i\varepsilon\alpha^2(\rho_o U_o^2) \tag{13}$$

On physical grounds, this "cut-off" distance $y_f$ represents the viscous displacement effect of the perturbation velocity field near the surface[9] as described below.

Various solutions of Eq. (11) have been studied previously. Lighthill[7] (1950) examined the general analytical structure of its two linearly independent solutions, and also discussed closed form asymptotic solutions in the limits of either small or large $\alpha\delta$ values. Application to a highly idealized wavy wall problem, wherein the boundary layer is approximated by a Mach number discontinuity so as to obtain a closed-form solution, was studied by Inger.[11] More detailed numerical solutions were subsequently obtained for a continuous Mach number distribution representative of a turbulent boundary-layer profile.[12] An important feature of the study was the development of a "top down" integration scheme whereby the split boundary-value problem for Eq. (11) is converted into an equivalent but more tractible initial value problem. In this scheme, a downward integration is initiated at $y = \delta$ from the known solution for uniform flow past wavy wall; then at any $0 \leqq y < \delta$ within the boundary layer, the resulting $\tilde{P}(y)$ defines a streamline via Eq. (3) to which an effective wavy wall of different amplitude and phase (relative to those at the outer edge) can be matched. By simply correcting for these amplitude and phase distortions, the true pressure signature on a wavy wall of amplitude $\varepsilon$ placed at the desired level can be determined. The inward march of this top down calculation is truncated at the effective wall position $y = y_f$.

Numerical interations of Eq. (11) by the aforementioned method have been obtained for turbulent boundary-layer Mach number profiles fitted to the present experiments using the theoretical model of Ref. 13 (see also Fig. 6). Figure 2 shows some typical variations of the pressure amplitude (relative to

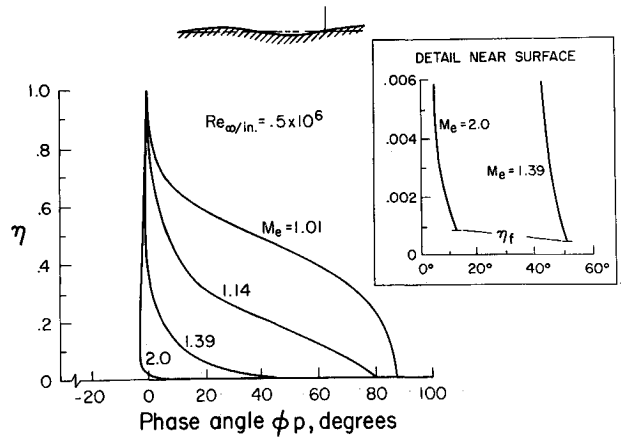


**Fig. 2 Theoretically predicted pressure phase variation across boundary layer.**

uniform potential flow) across the boundary layer, including details of the behavior near the surface. It is seen that the non-uniform velocity field causes a large decrease of the amplitude across the boundary layer at transonic edge Mach numbers. It is noted that, in agreement with predictions of the simplified model solution,[11] there is a negligible amplitude change across the layer when $M_e \approx 2^{1/2}$. Figure 3 illustrates the corresponding pressure phase variations across the boundary layer. A significant shift of pressure maximum toward the wavy wall valley is seen to occur as a result of the wave reflections from the boundary-layer profile when $M_e < 2$. Consequently, a subsonic type of pressure signature can exist on a wavy wall when the external inviscid flow is weakly to moderately supersonic.

### 2.3 Viscous and Heat Conduction Effects

We now consider the solution of the full Eqs. (1–5). Rather than carrying out a numerical investigation of this formidable set of equations, in the present work we shall seek an approximate analytical solution which brings out the essential physical features of the problem. To this end, we introduce the following simplifying assumptions: a) viscous dissipation heating effects on both the mean and perturbed flows are neglected, which is consistent with the already-accepted limitation to moderate supersonic Mach numbers[10,14]; b) under the high Reynolds number flow conditions of practical interest, viscosity and heat conduction effects on the perturbation field lie within a thin frictional sublayer whose thickness $\delta_f$ is small compared to the boundary-layer thickness $\delta$; c) in the case of turbulent motion, this friction sublayer lies within the so-called laminar sublayer such that the mean velocity and temperature profiles are approximately linear; d) the frictional sublayer is also small compared to the disturbance wavelength such that $(\alpha\delta_f)^2 \ll 1$, which is usually true for conditions of practical interest; e) compressibility effects on both the mean and disturbed flows are neglected, which again should be a reasonable approximation up to moderate supersonic Mach numbers provided the surface is not too highly cooled[14,15]; f) in turbulent flow the correlations between the disturbance field and the turbulent fluctuations are assumed negligible, thereby permitting the turbulent case to be treated as a "quasi-laminar" mean flow with an approximate eddy viscosity model. This undoubtedly introduces some quantitative errors except for very small disturbance amplitudes,[6] but these at present are difficult to estimate.

Under these assumptions, Eqs. (1–5) greatly simplify to the following:

$$i\alpha\tilde{U} + (d\tilde{V}/dy) \simeq 0 \tag{14}$$

$$i\alpha\rho_o(\tau_o/\mu_o)y\tilde{U} + \rho_o(\tau_o/\mu_o)V + i\alpha\tilde{P} \simeq \nu_o(d^2\tilde{U}/dy^2) \tag{15}$$

$$i\alpha(\tau_o/\mu_o)y\tilde{H} + (d\tilde{H}_o/dy)V \simeq \nu_o(d^2H/dy^2) \tag{16}$$

with $d\tilde{P}/dy \simeq 0$, (i.e., $\tilde{P}$ is constant across the friction layer as determined by the inviscid solution described above) and where $\tau_o/\mu_o = dU_o/dy$, $\rho_{o,w}$ and $\nu_{o,w}$ are the assumed constant mean flow velocity gradient, density and kinematic viscosity, respectively. Note that Eqs. (14) and (15) are uncoupled from the energy equation (16). The outer boundary conditions to impose are that the viscous parts of the solutions for $\tilde{U}$, $\tilde{V}$, and $\tilde{H}$ decay exponentially as $y \gg \delta_f$, whereas the inner boundary conditions are given by Eqs. (8–10) with $\mu(0) \simeq 0$ in Eq. (10b).

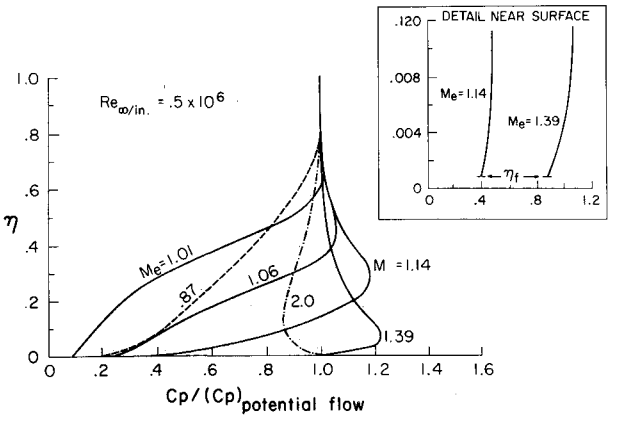


**Fig. 3 Theoretically predicted pressure amplitude variation.**

The solution for the velocity perturbation field is obtained as follows. Combining Eqs. (14–16) by differentiation of Eq. (15) so as to eliminate $\tilde{U}$ and $\tilde{P}$, we obtained an Orr-Sommerfeld equation for V alone:

$$\left\{i\alpha\left(\frac{\tau_o}{\mu_o}\right)y - \nu_o\frac{d^2}{dy^2}\right\}\frac{d^2\tilde{V}}{dy^2} = 0 \tag{17}$$

from which it is immediately seen that the characteristic thickness of the frictional sublayer must be $\delta_f = (\mu_o^2/\rho_o\tau_o\alpha)^{1/3}$. Introducing $\zeta = y/\delta_f$, Eq. (17) assumes the form of an Airy equation in $d^2V/d\zeta^2$, whose solution is of the form $\tilde{V} = A + B\zeta + c\chi(\zeta)$ where

$$\chi(\zeta) \equiv \int_\infty^\zeta \left\{\int_\infty^\zeta \zeta^{1/2}H_{1/3}^{(1)}\left[\frac{2}{3}(i\zeta)^{3/2}\right]d\zeta\right\}d\zeta \tag{18}$$

is the exponentially-decaying viscous part involving the Hankel function $H_{1/3}$ that has the properties $\chi(\infty) = 0$ and $\chi(0) = \frac{2}{3}$, $\chi'(0)/\chi(0) = -1.29\exp(\pi i/6)$, $\chi''(0)/\chi'(0) = -1.067\exp(\pi i/6)$ and $\chi'''(0)/\chi''(0) = -0.729i\exp(-\pi i/3)$. Application of the inner boundary conditions serves to determine the constants $A$ and $B$ and thereby to re-express $\tilde{V}$ in terms of the single constant $C = -c\chi'(0)$ as

$$\tilde{V} = \varepsilon\alpha U_o(y) + C\{\zeta - 0.776e^{-\pi i/6} - [\chi(\zeta)/\chi'(0)]\} \tag{19}$$

The first term on the right is the inviscid part of the solution which satisfies the kinematic tangency condition on a wavy wall placed a distance $y$ above the mean surface. The second term represents the viscous effect; as shown by Lighthill,[8] when viewed from a "large" distance $\zeta \gg 1$ (where $\chi \to 0$), this term vanishes at $\zeta_f = 0.776\exp(-\pi i/6)$, which defines the effective friction sublayer thickness as

$$y_f = 0.776(\mu_o^2/\rho_o\tau_o\alpha)^{1/3} \tag{20}$$

Equation (20) provides the required cut-off distance for the inviscid solution discussed earlier; note that it decreases as the one-third power of the surface ripple frequency and the mean shear stress. Evaluation of the constant $C$ and thereby the wall shear perturbation is accomplished by matching the viscous and inviscid values of $\tilde{U}$ at $y = y_f$. Assuming a linear mean flow velocity profile, this yields $C = 1.29\ i\varepsilon\alpha\delta_f(\tau_o/\mu_o)r_p\exp(\pi i/6)$ where $r_p = \alpha\delta_f^2\tilde{p}(y_f)/\varepsilon\tau$ is the ratio of pressure to viscous forces in the perturbation field. Equations (14) and (19) then give the shear stress perturbation as

$$\mu_o\frac{d\tilde{U}}{dy}(0) = \mu_o\frac{i}{\alpha}\frac{d^2\tilde{V}}{dy^2}(0) \simeq 1.37\left(\frac{\varepsilon}{\delta_f}\right)\tau_o r_p\exp\left(\frac{4\pi i}{3}\right) \tag{21}$$

whose phase lags the pressure by 120°.

We now consider energy transfer within the friction sublayer, a feature of the sinusoidal perturbation problem heretofore ignored in the literature. Appropriate to the present experiments, we treat the case of a fixed (small) mean heat transfer rate and seek the resulting surface temperature perturbation. It is convenient to recast Eq. (16) in terms of a new enthalpy variable defined by $\tilde{H}^* \equiv \tilde{H} - C_o\tilde{U}$ where $C_o = (dH_o/dy)_w/(dU_o/dy)_w$ is a Reynolds analogy factor. Then assuming the mean flow obeys the Crocco relation $H_o(y) = H_{o_w} + C_oU_o(y)$, multiplying Eq. (15) by $C_o$ and subtracting the result from Eq. (16) yields

$$\{i\alpha(\tau_o/\mu_o)y - \nu_o(d^2/dy^2)\}\tilde{H}^* = (i\alpha C_o\tilde{P}/\rho_o) \tag{22}$$

The appropriate boundary condition on $\tilde{H}^*$ at large $\zeta$ is that

$$\tilde{H}^* = \tilde{H}^*_{\text{inviscid}} \simeq [C_o\tilde{P}/(\tau_{o_w}y/\nu_o)] = (\alpha\delta_f^2C_o\tilde{P}/\mu_o) \tag{23a}$$

as inferred from Eq. (12), whereas at the wall we have from Eq. (10b) with $\tilde{u}(0) \simeq 0$ that

$$(d\tilde{H}^*/dy)(0) = C_o(d\tilde{U}/dy)(0) \tag{23b}$$

Now a comparison of Eqs. (22) and (16) shows that the

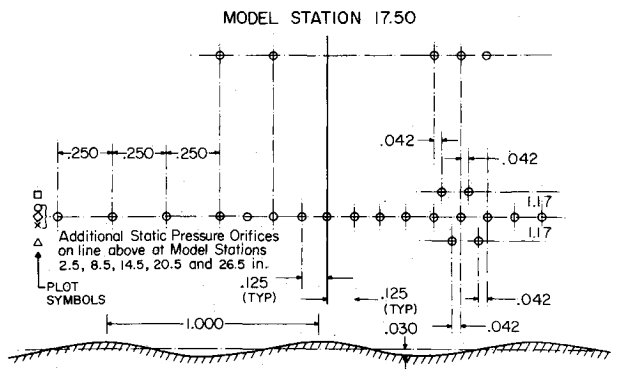


**Fig. 4 Pressure orifice locations on wavy wall model.**

complementary homogeneous solution of the former is proportional to $\tilde{V}'' \sim \chi''$. Furthermore, taking $\tilde{P} \simeq$ const, a particular integral of Eq. (22) that satisfies Eq. (23a) can be readily found in terms of a function $G$ studied some years ago by Holstein.[16] Consequently the complete solution can be written

$$\tilde{H}^* = D\chi''(\zeta) + [\alpha\delta_f{}^2 C_o \tilde{P}(y_f)/\mu_o]G(\zeta) \qquad (24)$$

where $D$ is a constant and $G \equiv \hat{G}'' + i\hat{H}''$ with $\hat{G}''$ and $\hat{H}''$ being functions defined and tabulated by Holstein such that $G(\zeta) = \zeta^{-1}$ as $\zeta \gg 1$, $G(0) = 1.285i$ and $G'(0) = 0.937$. Application of boundary condition (23b) and Eq. (21) serves to determine $D$ and thereby the following final result for the complex wall enthalpy perturbation:

$$\tilde{H}(0) = \tilde{H}^*(0) + i\varepsilon(dH_o/dy) = 0.595\varepsilon(dH_o/dy)r_p \exp(7\pi i/6) \qquad (25)$$

which is proportional to the mean flow heat-transfer rate. For the present experiments where the wavy wall was warmer than the local freestream total temperature, $dH_o/dy(0)$ is small and slightly negative. Equation (25) then predicts that the resulting surface temperature perturbation leads the pressure by 30° and hence that there is a strong correlation between the wall temperature and pressure disturbance peaks. This is corroborated by our temperature-sensitive liquid crystal paint observations, as discussed below.

Summarizing the present results on the relative phasing of the surface pressure, shear and temperature perturbations, there are two physical extremes: the first pertains to either subsonic external flow or supersonic external flow with a relatively thick boundary layer $\alpha\delta \gg 1$ such that the flow near the wall is effectively subsonic, while the second pertains to supersonic external flow with $\alpha\delta \gg 1$ such that the pressure field is effectively an inviscid supersonic one. In the former regime, the pressure and shear maxima occur in the surface valleys and near the crests, respectively, in qualitative agreement with Benjamin's analysis[9] whereas in the latter regime, these maxima have shifted 90° so as to place the pressure in its linearized supersonic position at the maximum surface slope.

## 3. Wavy Wall Experiment

### 3.1 Wind Tunnel, Model and Instrumentation

The purpose of this experiment was to measure the pressure and temperature along a simulated doubly infinite sinusoidal surface in the presence of a fully developed turbulent boundary layer at high subsonic and low supersonic speeds. It was carried out in the Douglas Aerophysics Laboratory Trisonic wind tunnel, a standard blowdown-to-atmosphere facility with a one foot square test section in which the Mach number is continuously variable from 0.3 to 1.25 and is obtainable from 1.4 to 3.5 by the use of fixed nozzle blocks. An aluminum wavy wall model replaced the entire vertical side wall and was centered about the transonic viewing window in the opposite side. The model incorporated a three cycle sine wave that spanned the test section from top to bottom normal to the wind-tunnel freestream flow. The wavy pattern had a one inch wavelength with an amplitude of 0.030 in. The transonic test section was used at all times, the remaining three walls being porous for the transonic runs but replaced with solid surfaces for the supersonic runs. Over-all, tests were conducted in a Mach number range from 0.9–1.8 with unit Reynolds numbers from 0.5–1.5 millions per inch.

The choice of the aforementioned wavy wall configuration was predicated on the following considerations. The number of ripples was chosen on the basis of McClure's results[6] that the anticipated flow requires about one cycle to adjust to an effectively locally sinusoidal behavior whereas more than about five cycles could cause incipient separation of the mean boundary layer; hence a three cycle configuration with most of the pressure taps on the last two was chosen as a reasonable compromise. The one inch wavelength arose from a desire to scale this length approximately to the local boundary-layer thickness (originally estimated at about 1 in.). The choice of amplitude presented an interesting trade-off problem A sufficiently large amplitude was desired to ease model fabrication tolerances and expense and also to optimize the accuracy of the pressure distribution measurements. On the other hand, it was deemed necessary to avoid separated flow, dictating a small amplitude. The amplitude of 0.030 in. chosen proved to be a good compromise for these purposes; separated flow occurred only once (the highest Mach number – lowest Reynolds number case) and then only on the aft wave.

The wavy wall was instrumented with thirty 0.030-in.-diam pressure taps as shown in Fig. 4. Rather than being uniformly spaced, these taps were located to measure the phase shift of the peak pressure and to determine if the pressure phasing is identical along two adjacent waves. Five scanivalves with five psi pressure transducers accurate to one percent were used to measure pressures on the model. Two data scans were made for all runs except the highest Reynolds number runs where the wind tunnel blow down times was limited to one scan. Each scan was initiated manually and required about 3 sec. Data from both scans agreed very well except for the one extreme high Mach number – low Reynolds number case where the flow appeared to be oscillating between attachment and separation of the aft wave (see discussion below). Further details on the experimental procedures are given in Ref. 17.

### 3.2 Temperature Sensitive Coatings

A novel aspect of the present tests was the use of liquid crystal paint to indicate the surface temperature distribution along the wavy wall. Liquid crystals have the advantage of reversibility, fast response and the ability to map finer details which cannot be derived from thermocouples even at far greater expense.[16] One thermocouple was also mounted at the top of the second sine wave with 0.01 in. of acrylic separating it from the boundary layer.

Since the highly-conductive aluminum of the basic wavy wall model was found to inhibit the surface temperature response

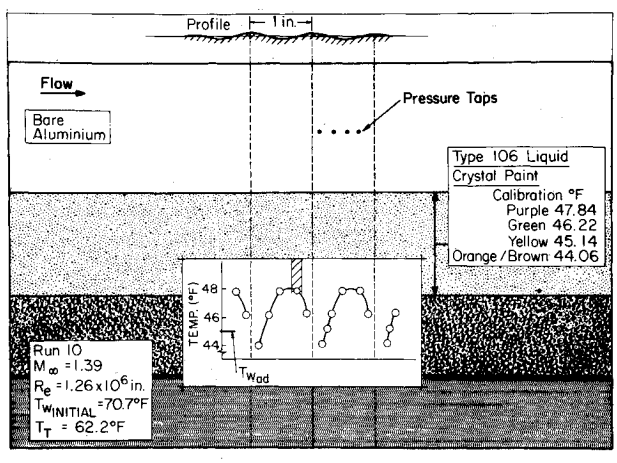


**Fig. 5 Liquid crystals on wavy wall model (schematic).**

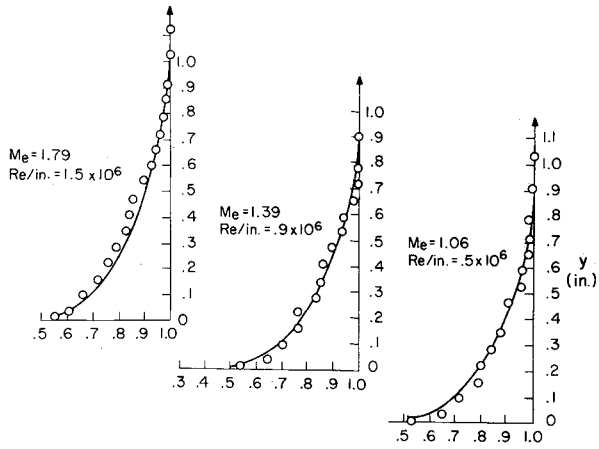


Fig. 6 Comparison of theoretical and experimental boundary-layer profiles.

of the liquid crystals, a 4-in. wide by 12-in. long acrylic insert painted flat black was used on one side of the model, opposite the pressure taps. Liquid crystals in a petroleum ether solution were applied uniformly to the insulated area with an artist's air brush. Three different types of crystals, each with a different band of temperature response in the range $38°F \leqq T_w \leqq 64°F$, were applied to the surface in parallel streamwise strips as illustrated in Fig. 5, where the pressure orifices can be seen in the aluminum surface above the liquid crystals (a color photograph of the actual surface during a run can be found in Ref. 17). It is noted that typical freestream total temperatures for these tests were lower than the corresponding wall recovery temperatures; consequently the wall was being cooled rather than being heated as in flight.

The temperature distributions on the sinusoidal surface were recorded with 35mm camera placed normal to the plane of the model. A single light source was used, its position being such as to minimize reflections from the model and the wind-tunnel windows. Prior to the test, the schlieren window was coated with magnesium fluoride to further reduce reflections from it.

### 3.3 Boundary-Layer Calibration Tests

Prior to the wavy wall tests, 29 calibration runs were made to measure the undisturbed boundary-layer profile and thickness in the transonic test section for each condition of the wavy wall test. These tests also served to check for any spanwise variation

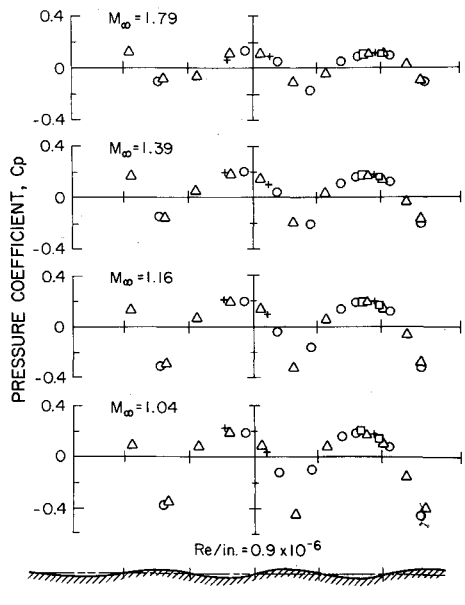


Fig. 7 Wavy wall pressure distributions at various Mach numbers.

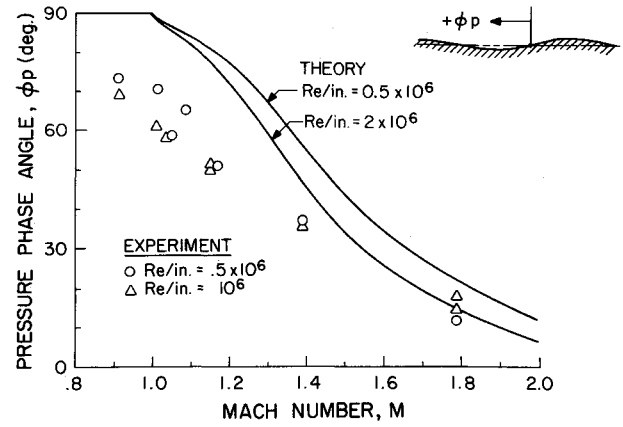


Fig. 8 Comparison of theoretical and experimental wall pressure shifts.

of boundary-layer properties and establish procedures for photographing the liquid crystal point. A standard twenty tube boundary-layer survey rake was located on the wall centerline with an alternate position two inches above. In addition, ten static pressure taps and three thermocouples were located on the wall giving a spanwise and a foreward streamwise survey originating at the rake. Pressure tubes from the rake and the wall were connected to 5 scanivalves located in the plenum chamber of the test section. The results of these surveys indicated that the spanwise variation of the boundary layer parameters around the test section centerline was insignificant in all cases. The typical centerline velocity profile was found to be fuller than a one-seventh power profile, indicating a well-developed turbulent boundary layer on the tunnel sidewall. Some typical experimental Mach number profiles and our corresponding analytical curve fits are illustrated in Fig. 6.

## 4. Discussion of Results

### 4.1 Pressure Distributions

Typical first-scan wall pressure distribution data for various Mach numbers are presented in Fig. 7. Different symbols are used to indicate the different spanwise pressure orifice locations denoted in Fig. 4: as expected, there was generally little change of pressure coefficient with span except in the one case where separated flow occured on the last wave. The first and second scan data were found to be virtually indistinguishable for all cases except $M_\infty = 1.79$ and $Re = 0.6 \times 10^6$/in., where separation was encountered accompanied by some spanwise pressure variation and fluctuation. An increase in unit Reynolds number eliminated this separation.

One of the principal objectives of the wavy wall tests was to check the theoretically-predicted phase shift in pressure across the boundary layer because of the nonuniform flow (simple uniform supersonic inviscid flow theory places the maximum pressure at the maximum wall slope point—the origin of the wavy wall pressure distribution plots in Fig. 7). A comparison of the theoretical and experimental phase shifts as a function of Mach number is given in Fig. 8. Qualitatively, the agreement is quite good as to trends with respect to both Mach and Reynolds number; quantitatively, the theory overestimates the phase shift angle by about 20° in the transonic regime.

A comparison of the corresponding results for pressure amplitude is presented in Fig. 9. It is seen that the magnitude of the pressure perturbation in the transonic regime is overestimated by the theory, although the main qualitative trends are again in good agreement with experiment. This is to be expected in view of the linearized nature of the analysis (note, however, that the inclusion of a nonuniform mean flow eliminates the $M = 1$ singularity otherwise associated with the linearized solution in uniform flow). Indeed, McClure[6] found that nonlinear effects were large enough even for only a three

percent amplitude ratio $\varepsilon/\lambda$ to reduce the peak pressures by as much as a factor of two, which is consistent with the present results. His data also agrees with ours in showing a decrease of this discrepancy with increasing Mach number.

An interesting feature of the present experiments is the occurrence of a pronounced nonsinusoidal variation or cusping at transonic speeds. Near Mach one, the absolute value of the negative pressure coefficient becomes double that of the positive pressure. This can be seen in Fig. 7 where this cusping trend is clearly illustrated. Since the spacing of static pressure orifices was chosen to define the phase shift of the peak positive pressure, the details of these unexpectedly cusped shapes are not too well defined. Some indication of this phenomenon is suggested by Hosokawa's analysis of transonic flow past a wavy wall.[3]

### 4.2 Surface Temperature Results

As discussed above (see Fig. 5), the surface temperature variation along the wavy wall was determined directly from color photographs of the liquid crystal response. Although the color changes spanwise are somewhat ragged, an oscillatory temperature variation in the streamwise direction was unmistakable. In Fig. 10 is shown a typical comparison of the corresponding wall temperature and pressure coefficient variations of a given run. Note that the pressure and temperature maxima very nearly coincide, in agreement with the theoretical prediction in Sect. 2. Although it is usually assumed without proof that the wall surface temperature disturbances are in phase with the corresponding pressure perturbations, this is the first time it has been theoretically proved and experimentally confirmed.

## 5. Conclusion

The significant results of this investigation can be summarized as follows.

1) Experiment and theory agree in showing that large changes in the phase of the pressure and temperature perturbations occur across the highly nonuniform flow of a turbulent boundary layer when the thickness is comparable to the surface wavelength. As a result, a subsonic wall pressure distribution can exist in the presence of a supersonic external inviscid flow.

2) The corresponding disturbance amplitudes also change significantly across the boundary layer, decreasing by 100% or more at the wall relative to the uniform inviscid flow value. The present linearized theory overestimates the experimental wall pressure by about a factor of two in the transonic regime owing to the appreciable nonlinear effects of the transonic regime that arise even at the very small (3%) wall amplitude of the present tests.

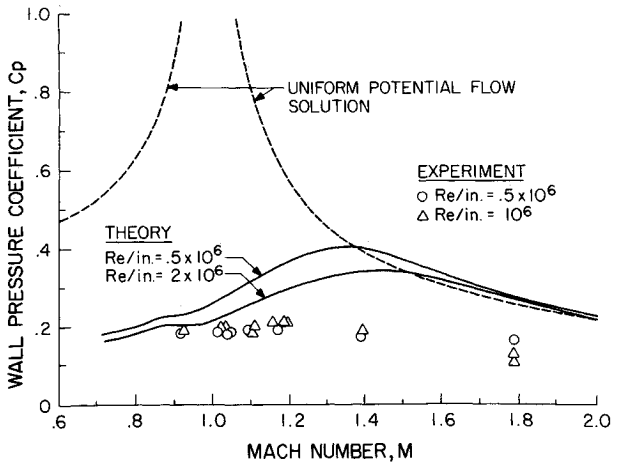


**Fig. 9 Comparison of theoretical and experimental wall pressures amplitudes.**

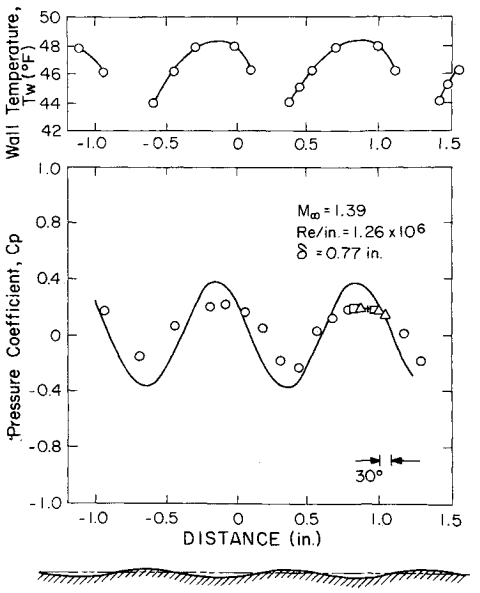


**Fig. 10 Typical correlation between pressure and temperature measurements.**

3) By a suitable generalization of Lighthill's earlier work[8] to include heat-transfer effects, it is predicted that the surface temperature and pressure maxima are closely correlated. This was experimentally verified by direct measurement of surface temperature variations along a nearly-adiabatic wavy wall coated with extremely temperature sensitive liquid crystal paint.

4) The experiments reveal the gradual appearance of a nonharmonic (but periodic) pressure distribution in the transonic regime near Mach one. In particular, a decided cusping of the pattern occurs which is apparently indicative of the locally imbedded supersonic regions very close to the surface.

On the basis of these findings, the following features of the problem warrant further investigation. a) An experimental study of the relative effects of wall amplitude and wavelength by means of systematic variations in the parameters $\varepsilon/\lambda$ and $\alpha\delta$ ranging from small to large values. This would include, for example, identification of the boundary-layer separation threshhold and the minimum $\varepsilon/\lambda$ required for linearized behavior. Correspondingly, it would be desireable to extend the present theory to include the nonlinear effects of perturbation feedback on the mean flow property profiles. b) Investigation of the pressure-temperature relationship in situations differing significantly from the present case of small negative surface heat transfer. These might include the case of a slightly cooled wall (using again liquid crystal paint) or the case of large surface heat transfer where heat-transfer gages could be used to measure heat-transfer perturbations. c) A more detailed study of the transonic anharmonic region and the relationship of the pressure cusping to the basic flow parameters. This would involve extending the present theory to include nonlinear transonic effects in a nonuniform boundary-layer flow.

## References

[1] Fannelop, T. and Flugge-Lotz, I., "The Laminar Compressible Boundary Layer Along a Wave-Shaped Wall," *Ingenieur Archiv*, Vol. 33, No. 1, Jan. 1963, pp. 24–35.

[2] Bertram, M. H., Weinstein, L. M., Cary, A. M., and Arrington, J. P., "Heat Transfer to Wavy Wall in Hypersonic Flow," *AIAA Journal*, Vol. 5, No. 10, Oct. 1967, pp. 1960–1967.

[3] Hosokawa, I., "Transonic Flow Past a Wavy Wall," *Journal Physical Society of Japan*, Vol. 15, No. 11, Nov. 1960, pp. 2080–2086.

[4] Larson, H. K. and Mateer, G. G., "Cross-Hatching—A Coupling of Gas Dynamics with the Ablation Process," AIAA Paper 68-670, Los Angeles, Calif., 1968.

[5] Nachtscheim, P. R., "Analysis of the Stability of a Thin Liquid Film Layer Adjacent to a High Speed Gas Stream," TN D-4976, Jan. 1969, NASA.

[6] McClure, J. D., "On Perturbed Boundary Layer Flows," Fluid Dynamic Research Lab. Rept. 62-2, July 1962, MIT, Cambridge, Mass.

[7] Lighthill, M. J., "Reflection at a Laminar Boundary Layer of a Weak Steady Disturbance to a Supersonic Stream, Neglecting Velocity and Heat Conduction," *Quarterly Journal of Mechanics and Applied Mathematics*, Vol. 3, No. 3, March 1950, pp. 302–325.

[8] Lighthill, M. J., "On Boundary Layers and Upstream Influence II Supersonic Flows Without Separation," *Proceedings of the Royal Society*, Vol. 217, 1953, pp. 478–507.

[9] Benjamin, T. B., "Shearing Flow Over a Wavy Boundary," *Journal of Fluid Mechanics*, Vol. 6, No. 2, 1959, pp. 161–205.

[10] Lees, L. and Reshotko, E., "Stability of the Compressible Laminar Boundary Layer," *Journal of Fluid Mechanics*, Vol. 12, No. 4, 1962, pp. 555–590.

[11] Inger, G. R., "Discontinuous Supersonic Flow Past an Ablating Wavy Wall," *AIAA Journal*, Vol. 7, No. 4, April 1969, pp. 762–764.

[12] Inger, G. R., "Rotational Inviscid Supersonic Flow Past a Wavy Wall," *Bulletin of the American Physical Society*, Vol. 13, No. 11, Nov. 1968, p. 1579.

[13] Martellucci, H., Rie, H., and J. F. Somtowski, J. F., "Evaluation of Several Eddy Viscosity Models through Comparison with Measurements in Hypersonic Flows," AIAA Paper 69-688, San Francisco, Calif., 1969.

[14] Brown, W. B., "Stability of Compressible Boundary Layers," *AIAA Journal*, Vol. 5, No. 10, Oct. 1967, pp. 1753–1759.

[15] Lew, H. G. and Li, H., "The Role of the Turbulent Viscous Sublayer in the Formation of Surface Patterns," Rept. R68SD12, June 1968, General Electric Missle and Space Div., Valley Forge, Pa.

[16] Klein, E. J., "Liquid Crystals in Aerodynamic Testing," *Astronautics and Aeronautics*, Vol. 6, No. 7, July 1968, pp. 20–25.

[17] Williams, E. P. and Inger, G. R., "Investigations of Ablation Surface Cross Hatching," SAMSO TR-70-246, June 1970, McDonnell Douglas Astronautics, Huntington Beach, Calif.

MAY 1972 AIAA JOURNAL VOL. 10, NO. 5

# Boundary-Layer Separation on Slender Cones at Angle of Attack

KENNETH F. STETSON*
*Aerospace Research Laboratories, Wright-Patterson Air Force Base, Ohio*

**Experimental results of hypersonic laminar boundary-layer separation on cones at angle of attack were obtained in a $M_\infty = 14.2$ wind tunnel with a 5.6° half-angle cone model with sharp and spherically blunt tips. Based on data consisting of surface pressure measurements, Pitot pressure surveys, and surface oil flow patterns, a new model for hypersonic three-dimensional separation is proposed. This model, for both sharp and blunt cones, contains symmetrical supersonic helical vortices with an attachment line on the most leeward ray and resembles Maskell's free vortex layer type of separation. For the blunt cone the separation lines appear to orginate in the region where the lateral component of skin friction is zero. The vortices are close to the surface (at least up to $\alpha = 18°$) and there is no subsonic reverse flow associated with the vortex pattern.**

## Nomenclature

$L$ = total model surface length
$M_\infty$ = freestream Mach number
$p_B$ = base pressure
$p$ = cone surface pressure
$p_\infty$ = freestream pressure
$p_o$ = wind-tunnel reservoir pressure
$p_{st}$ = stagnation pressure on model
$p_{T_2}$ = Pitot pressure
$r$ = radial distance from center of model base
$Re_\infty$/ft = unit Reynolds number based on freestream conditions
$R_B$ = model base radius
$R_N$ = nose radius
$T_o$ = wind-tunnel reservoir temperature
$X$ = distance along the cone surface from the tip or from the zero angle-of-attack stagnation point
$\alpha$ = angle of attack
$\theta_c$ = cone half-angle
$\phi$ = cone circumferential angle, measured in a clockwise direction based on a head-on view, with the most windward ray being designated $\phi = 0$

Presented as Paper 71-129 at the AIAA 9th Aerospace Sciences Meeting, New York, January 25–27, 1971; submitted June 3, 1971; revision received December 27, 1971.

Index categories: Boundary Layers and Convective Heat Transfer—Laminar; Supersonic and Hypersonic Flow; Jets, Wakes, and Viscid-Inviscid Flow Interactions.

* Aerospace Engineer, Fluid Dynamics Facilities Research Laboratory. Associate Fellow AIAA.

## Introduction

THE leeward region of a slender body at angle of attack has associated with it a complex viscous-inviscid interaction and may include a three-dimensional separated flowfield. Considerable progress has been made in calculating three-dimensional flowfields about cones at angle of attack for the case of an attached boundary layer[1–6]; however, these techniques have not proven capable of making an adequate prediction of boundary-layer separation or producing a solution downstream of separation. Limited experimental data[7–12] have only partially defined the leeward flowfield characteristics. Although these investigations had significantly increased the general understanding of flowfields about cones at angle of attack, it was not possible from these findings to establish an appropriate flowfield model for three-dimensional separation.

Maskell[13] has identified several possible models for three-dimensional separation on a body of revolution at angle of attack; however, their occurrence in given physical situations remains to be determined. The three-dimensional separation bubble has been considered by many investigators to be the most likely flowfield model for separation on a blunt cone at angle of attack. A pictorial representation of this model of separation is shown in Fig. 1. Significant features of this model are a separation line which originates from a singular point on the most leeward generator and a separated layer enclosing a "bubble". Upstream of the separation bubble the leeward flowfield is nose-dominated, with large favorable pressure gradients, and the boundary layer is attached. The bubble contains subsonic flow traveling upstream